Global Nonlinear Solutions in Sequence Space and the Generalized Transition Function[1]

Online Appendix

Contents

[1]Hanbaek Lee, University of Cambridge, Email: hanbaeklee1@gmail.com

A Implementation of the repeated transition method

A.1 Implementation

The method starts from simulating a single path of exogenous aggregate shocks for a long-enough period T, $\mathbb{S} = \{S_t\}_{t=0}^{T}$, using the aggregate transition matrix Π^S. A time partition $\mathcal{T}(S)$ is defined as group of periods that share the same aggregate exogenous state realization as follows.

$$\mathcal{T}_S := \{\tau | S_\tau = S\} \subseteq \{0, 1, 2, ..., T\} \text{ for } S \in \{B, G\}.$$

The pseudo algorithm of the RTM is as follows:

Step 1. Guess on the paths of the value functions, the endogenous states, and the prices:[2]

$$\{V_t^{(n)}, \Phi_t^{(n)}, p_t^{(n)}\}_{t=0}^{T}.$$

Step 2. Solve the model backward from the terminal period T in the following sub-steps. The explanation is based on an arbitrary period t. For an illustrative purpose, I assume $S_t = G$ and $S_{t+1} = G$:

2-a. Find $\widetilde{t}+1$ where the endogenous aggregate allocation in period is identical to the one in period $t+1$, but the shock realization is different from period $t+1$ ($S_{\widetilde{t}+1} = B$):[3]

$$\widetilde{t}+1 = \arg \inf_{\tau \in \mathcal{T}_B} ||\Phi_\tau^{(n)} - \Phi_{t+1}^{(n)}||_\infty.$$

2-b. Compute the expected future value function as follows:

$$\mathbb{E}_t \widetilde{V}_{t+1} = \pi_{G,G} V_{t+1}^{(n)} + \pi_{G,B} V_{\widetilde{t}+1}^{(n)}.$$

2-c. Using $\mathbb{E}_t \widetilde{V}_{t+1}$ and $p_t^{(n)}$, solve the individual agent's problem at the period t. Then, I obtain the solution $\{V_t^*, a_{t+1}^*\}$.

After the taking these sub-steps for $\forall t$, $\{V_t^*, a_{t+1}^*\}_{t=0}^{T}$ are available.

[2] In practice, I use the stationary equilibrium allocations for all periods as the initial guess.

[3] Such $\widetilde{t}+1$ might not be unique. However, any of such $\widetilde{t}+1$ is equally good to be used in the next step.

Step 3. Using $\{a^*_{t+1}\}_{t=0}^T$, simulate forward the time series of the endogenous states $\{\Phi^*_t\}_{t=0}^T$ starting from $\Phi^*_0 = \Phi^{(n)}_0$.[4]

Step 4. Using $\{\Phi^*_t\}_{t=0}^T$, all the aggregate allocations over the whole path such as $\{K^*_t\}_{t=0}^T$ can be obtained. Using the market-clearing condition, compute the time series of the market-clearing price. If the model features a non-trivial market clearing condition, compute the time series of the implied prices $\{p^*_t\}_{t=0}^T$.[5]

Step 5. Check the distance between the implied prices and the guessed prices.

$$\sup_{BurnIn \leq t \leq T-BurnIn} ||p^*_t - p^{(n)}_t||_\infty < tol$$

Note that the distance is measured after excluding the burn-in periods at the beginning and the end of the simulated path. This is an adjustment to handle a potential bias from the imperfect guesses on the terminal period's value function $V^{(n)}_T$ and the initial period's endogenous state $\Phi^{(n)}_0$. The convergence criterion can be augmented by including the distance in other allocations, such as value functions or endogenous states.

If the distance is smaller than the tolerance level, the algorithm is converged. Otherwise, I make the following updates on the guess:[6]

$$p^{(n+1)}_t = p^{(n)}_t \psi_1 + p^*_t (1 - \psi_1)$$

$$V^{(n+1)}_t = V^{(n)}_t \psi_2 + V^*_t (1 - \psi_2)$$

$$\Phi^{(n+1)}_t = \Phi^{(n)}_t \psi_3 + \Phi^*_t (1 - \psi_3)$$

[4] In this step, if the endogenous state is a distribution, I use the non-stochastic simulation method (Young, 2010).

[5] It is worth noting that the prices here are not the market-clearing prices that are determined from the interactions between demand and supply. Rather, they are the prices implied by the market-clearing condition given either demand or supply fixed at the n^{th} iteration:

$$p^*_t = \arg_{\widetilde{p}}\{Q^D(p^{(n)}_t, X_t, X_{t+1}) - Q^S(\widetilde{p}, X_t, X_{t+1}) = 0\} \text{ or}$$
$$p^*_t = \arg_{\widetilde{p}}\{Q^D(\widetilde{p}, X_t, X_{t+1}) - Q^S(p^{(n)}_t, X_t, X_{t+1}) = 0\}.$$

In the computation method used in Krusell and Smith (1997), a market-clearing price needs to be computed in an additional loop due to the non-trivial market-clearing condition. The implied price cannot replace the market-clearing price in this method, as the misspecified price prediction rule can lead to a divergent law of motion of the aggregate allocation. In contrast, due to the missing market clearing step, the RTM significantly saves computation time.

[6] In highly nonlinear aggregate dynamics, I have found that the log-convex combination updating rule marginally dominates the standard convex combination updating rule in terms of convergence speed. The log-convex combination rule is as follows:

$$log(p^{(n+1)}_t) = log(p^{(n)}_t)\psi_1 + log(p^*_t)(1 - \psi_1).$$

for $\forall t \in \{0, 1, 2, 3, ..., T\}$. With the updated guess $\{V_t^{(n+1)}, \Phi_t^{(n+1)}, p_t^{(n+1)}\}_{t=0}^{T}$, I go back to Step 1.

(ψ_1, ψ_2, ψ_3) are the parameters of convergence speed in the algorithm. If ψ_i is high, then the algorithm conservatively updates the guess, leaving the algorithm to converge slowly. If the equilibrium dynamics are almost linear, as in Krusell and Smith (1998), uniformly setting ψ_i at around 0.9 guarantees convergence at a fairly high convergence speed. However, if a model is highly nonlinear, the convergence speed needs to be controlled to be substantially slower than the one in the linear models. This is because the nonlinearity can lead to a sudden jump in the realized allocations during the iteration if a new guess is too dramatically changed from the last guess. A heterogeneous updating rule $\psi_i \neq \psi_j$ $(i \neq j)$ is also helpful in cases where the dynamics of certain allocations are particularly more nonlinear than the others.

Depending on the models, the guessed bundle can include the paths of the optimal decision rules on top of the basic three allocations. For example, in an application for a global nonlinear solution for the canonical New Keynesian model with Rotemberg price adjustment cost, the paths of labor demand and consumption are all included in the bundle of guess and simultaneously updated with the inter-temporal policy functions, endogenous states, and prices.[7]

As can be seen from the convergence criterion in Step 5, the algorithm stops when the predicted allocation paths (n^{th} iteration) are close enough to the realized allocation paths (with asterisks). Therefore, once the convergence is achieved, the solution is guaranteed to be dynamically consistent: the predicted path coincides with the realized path. If the accuracy is measured in R^2 or in the mean-squared errors, as in Krusell and Smith (1998), the RTM features R^2 at 1, and its mean-squared error becomes negligibly different than zero.

A.2 The required length of simulation path

In this section, I discuss how long a simulation needs to be for the RTM. First, one of the most crucial determinants of the desired length is the assumed Markov process of the exogenous aggregate states. That is, the number of realizations of each exogenous state during the simulation is the key information. As in Krusell and Smith (1998), if only two aggregate states are realized based on a symmetric transition probability of a moderate level (0.875), the simulation of 500 periods is good enough to make the solution stay unaffected by further lengthening. However, for models

[7] The sample code and the model elaboration is available in the Online Appendix.

with more complex exogenous state processes, a longer simulation may be required. If an aggregate TFP process is discretized by the Tauchen method, covering three standard deviation ranges, at least 3,000 periods are needed to have enough realizations (at least 30) for both ends of the grids. The persistence of the exogenous state process also plays a role, with greater persistence requiring longer simulation periods.[8]

The nonlinearity of the model is another critical factor in determining the required simulation length. In practice, the RTM groups periods with similar endogenous aggregate states and uses piecewise interpolation to fill in missing observations. For highly nonlinear DSGE models, having additional observations in each exogenous state realization can substantially improve the accuracy of the solution by providing more nodes for interpolation. In the case of the highly nonlinear RBC model with irreversible investment, increasing the simulation length gradually changes the solutions until 4,000 periods are reached, after which the solution remains unaffected by additional periods.

While the required simulation length for the RTM is not necessarily longer than that used in the state space-based approach, it varies depending on the shock's persistence and the model's nonlinearity. The accuracy of the RTM stems from its ability to update the entire predicted path of allocations based on the entire realized path, which maximizes the information passed on to the next iteration. This contrasts with the state space-based approach, which relies on a functional relationship between the current and future periods that only summarily captures the dynamics. As a result, the RTM can achieve high accuracy without requiring a particularly longer simulation period compared to alternative methods.

A.3 Implementation of the sufficient statistic approach

In the algorithm explained in the previous section, Step 2-a is the most demanding step for heterogeneous-agent models, as it needs to find a period $\widetilde{t}+1$ that is identical to period $t+1$ in terms of distribution. Therefore, the similarity of the distributions across the periods needs to be measured, which is computationally costly.

However, if there is a sufficient statistic that can perfectly represent a period's endogenous aggregate state, the computational efficiency can be substantially improved. This enables to locate the target period $\widetilde{t}+1$ by only comparing the distance between these sufficient statistics instead of the distributions. For example, in Krusell and Smith (1998), if the aggregate capital is the sufficient

[8] It is important to note that the RTM is not unique in its sensitivity to simulation length. Other approaches, such as the state space-based approach, also require a sufficient number of observations in each exogenous state realization to ensure accuracy.

statistic, Step 2-a becomes easier as follows:

$$\widetilde{t}+1 = \arg \inf_{\tau \in \mathcal{T}_B} ||K_{\tau}^{(n)} - K_{t+1}^{(n)}||_{\infty}.$$

As the algorithm relies on the ergodicity, a sufficiently long period of simulation is needed for accurate computation. However, in practice, the simulation ends in finite periods. Therefore, the period $\widetilde{t}+1$ that shares exactly identical sufficient statistic as period t+1 might not exist. For this hurdle, the following adjusted versions of Step 2-a and Step 2-b help improve the accuracy of the solution:

2-a′. Find $\widetilde{t}^{up}+1$ where the sufficient statistic of the endogenous aggregate state is closest to the one in period $t+1$ from above, but the shock realization is different from period $t+1$:

$$\widetilde{t}^{up}+1 = \arg \inf_{\tau \in \mathcal{T}_B \text{ s.t. } e_{\tau}^{(n)} \geq e_{t+1}^{(n)}} ||e_{\tau}^{(n)} - e_{t+1}^{(n)}||_{\infty},$$

where e_{τ} denotes the sufficient statistic of the endogenous aggregate state in period τ. Similarly, find $\widetilde{t}^{dn}+1$ where the sufficient statistic of the endogenous aggregate state is closest to the one in period $t+1$ from below, but the shock realization is different from period $t+1$:

$$\widetilde{t}^{dn}+1 = \arg \inf_{\tau \in \mathcal{T}_B \text{ s.t. } e_{\tau}^{(n)} < e_{t+1}^{(n)}} ||e_{\tau}^{(n)} - e_{t+1}^{(n)}||_{\infty}.$$

Then, I have $e^{(n)}_{\widetilde{t}^{up}+1}$ and $e^{(n)}_{\widetilde{t}^{dn}+1}$ that are closest to $e^{(n)}_{t+1}$ from above and below, respectively. Using these two, I compute the weight ω to be used in the convex combination of value functions in the next step:

$$\omega = \frac{e_{t+1}^{(n)} - e^{(n)}_{\widetilde{t}^{dn}+1}}{e^{(n)}_{\widetilde{t}^{up}+1} - e^{(n)}_{\widetilde{t}^{dn}+1}}.$$

2-b′. Compute the expected future value function as follows:

$$\mathbb{E}_t \widetilde{V}_{t+1} = \pi_{G,G} V_{t+1}^{(n)} + \pi_{G,B} \left(\omega V^{(n)}_{\widetilde{t}^{up}+1} + (1-\omega) V^{(n)}_{\widetilde{t}^{dn}+1} \right).$$

Step 2-a' and Step 2-b' construct a synthetic counterfactual conditional value function by the

convex combination of the two value functions that are for the most similar periods to period $t+1$. These adjusted steps help accurately solve the problem in relatively short periods of simulation. For example, the model in Krusell and Smith (1998) can be accurately solved using only $T = 500$ periods of simulation (except for 100 burn-in periods at the beginning and the end of the simulated path).

The step of interpolation after finding the closest periods in terms of sufficient statistics can be understood as a piecewise interpolation, in contrast to the unconditional linear interpolation used in the state space-based approach based on the regression coefficients.

B The method's performance comparison: accuracy

This section compares the RTM's computational performance against existing global solution methods for heterogeneous-agent models. Especially it evaluates the RTM's performance in two settings: the heterogeneous-household model of Krusell and Smith (1998) comparing against Maliar et al. (2010), and the heterogeneous-firm model of Khan and Thomas (2008), benchmarking against their original Krusell and Smith (1997) solution approach.[9]

The RTM demonstrates particularly substantial computational advantages in models featuring non-trivial market clearing conditions. For example, when solving the Khan and Thomas (2008) model, the RTM converges approximately ten times faster than the Krusell and Smith (1997) algorithm. This efficiency gain stems from a fundamental methodological difference: while state-space-based approaches require computationally expensive nested loops to find exact market clearing prices in each period, the RTM employs implied prices that naturally converge to market clearing values through iteration. This approach eliminates the need for nested fixed-point calculations while maintaining solution accuracy. However, it's important to note that when the RTM is applied to a heterogeneous-agent model as in Krusell and Smith (1998) without the non-trivial market clearing condition, the RTM's computational efficiency is similar to Maliar et al. (2010).

Then, I compare the repeated transition method with the other nonlinear solution methods in the literature for three DSGE models. The comparison is based on a real business cycle model with irreversible investment (McGrattan, 1996; Christiano and Fisher, 2000), where I benchmark the RTM against three alternatives: linearized solution, the OccBin method of Guerrieri and Iacoviello (2015) and the GDSGE solution of Cao et al. (2023).

Consider a representative household solving the following problem:

$$V(a;X) = \max_{c,a'} \frac{c^{1-\sigma}}{1-\sigma} + \beta \mathbb{E} V(a';X') \tag{1}$$

$$\text{s.t. } c + a' - (1-\delta)a = Aa^{\alpha} \tag{2}$$

$$a' - (1-\delta)a \geq \phi I_{ss} \tag{3}$$

where V is the value function of a household. The value function's arguments are wealth a and the aggregate state X. c is consumption and σ is the risk-aversion parameter. I_{ss} is the steady-state investment level. ϕ is the parameter for the degree of the irreversibility. δ is the depreciation

[9] All computations use a MacBook Pro 2021 with M1 Pro chip.

rate, and α is the capital share in the production function $F(a; A) := Aa^{\alpha}$. Apostrophes denote next-period variables. The aggregate state X is as follows

$$X = [K, A]. \tag{4}$$

K is the aggregate capital stock, satisfying $a = K$ in equilibrium, as the capital market clears. A is TFP that follows the log AR(1) process:

$$log(A') = \rho log(A) + \sigma\epsilon, \quad \sigma \sim N(0, 1). \tag{5}$$

The model features highly nonlinear aggregate dynamics due to the occasionally binding irreversibility constraint for capital investment. Therefore, besides the macroeconomic implications, the model serves as an ideal testing ground for the accuracy of the different methods for the nonlinear solutions. For precise comparison, I generate a single TFP path using the Tauchen method (7 grid points covering three standard deviations) and apply this path to all solution methods. The simulation runs for 5,000 periods with 500 burn-in periods. Each method exhibits a trade-off between accuracy and computational efficiency depending on convergence criteria. In this comparison, I tune the repeated transition method to stop after around 90 seconds, matching the speed of the GDSGE toolkit.

The first four rows of Table B.1 compare solution accuracy across methods, with columns presenting results for the RTM, GDSGE, OccBin, and linearized solutions, respectively. I evaluate accuracy using two criteria: dynamic consistency error ($Error_t$) and Euler equation error (EE_t) following Judd (1992).[10] The dynamic consistency error is defined as:

$$Error_t = K_t^{(n)} - K_t^* \tag{6}$$

where $\{K_t^{(n)}\}_{t=1}^T$ represents the capital stock sequence from each solution method, and K_t^* is the implied capital path assuming agents expect $\{K_t^{(n)}\}_{t=1}^T$. The RTM constructs the period-specific expected future allocations by properly combining allocations in the predicted path (the previous iteration). Then, it provides the realized allocations implied by the prediction path. Dynamic consistency requires these predicted and realized paths to coincide. Thus, the RTM to serve as a diagnostic tool for other solution methods - by feeding their simulated paths as predicted paths

[10]The Euler equation error specification follows Guerrieri and Iacoviello (2015).

into the RTM algorithm, the RTM can evaluate their dynamic consistency.

Table B.1: Comparison across the solution methods

	RTM	GDSGE	OccBin	Linear
Accuracy				
$max(\|Error_t\|)$ (% of steady-state K)	0.003	0.735	1.317	2.019
$\sqrt{mean(Error_t^2)}$ (% of steady-state K)	0.001	0.025	0.217	0.559
$max(\|EE_t\|)$ (% of contemp. C_t)	0.014	0.057	2.854	2.323
$\sqrt{mean(EE_t^2)}$ (% of contemp. C_t)	0.002	0.059	0.775	0.707
Business cycle stat.				
$mean(I)$	0.363	0.363	0.365	0.363
$mean(C)$	1.166	1.166	1.164	1.160
$vol(I)$	0.022	0.022	0.023	0.023
$vol(C)$	0.052	0.052	0.052	0.052
$skewness(I)$	1.363	1.320	1.307	1.407
$skewness(C)$	-0.225	-0.213	-0.322	-0.095
$kurtosis(I)$	4.447	4.578	4.513	4.255
$kurtosis(C)$	2.776	2.546	2.858	2.796

Notes: The upper part of the table compares the accuracy of different computation methods based on four criteria: 1) maximum absolute prediction error, 2) square root of mean squared prediction error, 3) maximum absolute Euler equation error, 4) square root of mean squared Euler equation error. The bottom part of the table compares the computed equilibrium's business statistics.

The RTM displays a higher accuracy than other methodology in terms of the four statistics: the absolute maxima of the dynamic inconsistency (first row) and the Euler equation error (third row); the square roots of the mean-squared dynamic inconsistency (second row) and the Euler equation error (fourth row).

The RTM achieves its accuracy and speed using standard MATLAB code, without relying on lower-level languages like C++ or advanced econometric techniques. The method's dynamic consistency error can theoretically be reduced to any arbitrary level by adjusting convergence tolerance, suggesting potential for further improvement through integration with lower-level programming languages or modern machine learning techniques (Azinovic et al., 2022; Fernández-Villaverde et al., 2023; Han et al., 2025).[11]

Table B.1's lower panel reports business cycle statistics across solutions. While lower-order moments show negligible differences, higher-order moments (skewness and kurtosis) reveal significant

[11]One potential synergy between the RTM and the advanced machine learning techniques is in the identification step for the target period from the previous iteration.

Figure B.1: The equilibrium path of different solutions

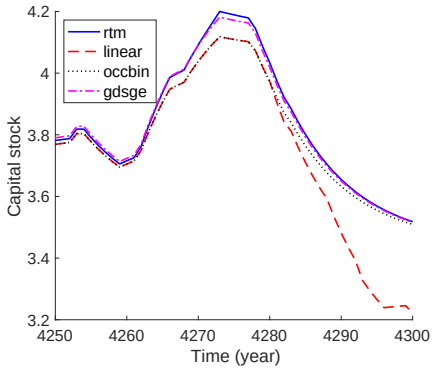

Notes: The figure plots a subsample of the equilibrium dynamics computed using four different methods. The solid line indicates the RTM; the dashed line is by linear method; the dotted line is by OccBin toolkit; and the dash-dotted line is by GDSGE method.

variations across methods. Figure B.1 illustrates these differences by plotting capital stock paths from each solution method. The RTM solution most closely matches the GDSGE toolkit, while the OccBin solution shows notable deviations, particularly when aggregate capital is high. The absolute difference between RTM and OccBin solutions correlates positively with output (correlation 0.631), indicating pro-cyclical computation error. Conversely, differences between RTM and linear solutions show counter-cyclical patterns (correlation -0.640). These patterns reflect each method's relative strength: OccBin provides more accurate solutions during downturns when constraints bind but less accurately captures precautionary behavior in normal times. The linear solution, by contrast, fundamentally struggles with occasionally binding constraints, leading to large errors during downturns.

C The method's performance comparison: Krusell and Smith (1998) and Khan and Thomas (2008)

This section compares the performance of the RTM with the existing methods based on the heterogeneous-agent models. First, I compare the equilibrium allocations obtained from the RTM and the ones from the method in Maliar et al. (2010) for the model of Krusell and Smith (1998).[12] The RTM computes the exact level of the Lagrange multiplier for the occasionally binding constraint at the individual level, which enables the accurate computation. The path of the lagrange multipliers is computed by the residuals using the Euler equation as in Rendahl (2014).[13] With both algorithms calibrated to converge in approximately two minutes, their accuracy in terms of square root dynamic consistency differs by less than 10^{-5}. This negligible difference, despite Maliar et al. (2010) not computing Lagrange multipliers for occasionally binding constraints, reflects a model characteristic: the total amount of wealth held by constrained households is negligibly small, not meaningfully contributing to the aggregate capital dynamics. The similar performance between the two algorithms is due to the linearity of the capital dynamics, which makes the state space-based approach and the sequence space-based approach only negligibly different. It takes around 20 minutes for the RTM to converge under the convergence speed parameter $\psi_1 = \psi_2 = \psi_3 = 0.8$, which is a similar computation speed as Maliar et al. (2010) algorithm.

Figure C.2 plots a part of the predicted path $\{K_t^{(n)}\}_{t=0}^T$ and the realized (implied) path $\{K_t^*\}_{t=0}^T$ of aggregate capital K_t obtained from the RTM and the simulated path from the fitted log-linear law of motion (Krusell and Smith, 1998).[14] As can be seen from all three lines hardly distinguished from each other, the RTM computes almost identical equilibrium allocations as the log-linear law of motion by Krusell and Smith (1998). This is because the log-linear specification almost perfectly captures the actual law of motion in the model.

However, when a model features a non-trivial market-clearing condition, as in the model of Khan and Thomas (2008), the RTM substantially outperforms the state space-based approach based on the law of motion Krusell and Smith (1997). This is because their method requires to include an extra loop to find an exact market clearing prices in each period, while the RTM avoids

[12] The parameters are set as in the benchmark model in Krusell and Smith (1998) without idiosyncratic shocks in the patience parameter β.

[13] For some models where an occasionally binding constraint includes the current individual/aggregate state (e.g., irreversible investment), it is necessary to compute the expected future Lagrange multipliers. The RTM can accurately compute this expectation. Section D.1 and D.2 provide further explanations.

[14] This figure is motivated from the fundamental accuracy plot suggested in Den Haan (2010).

Figure C.2: Equilibrium aggregate capital dynamics (Krusell and Smith, 1998)

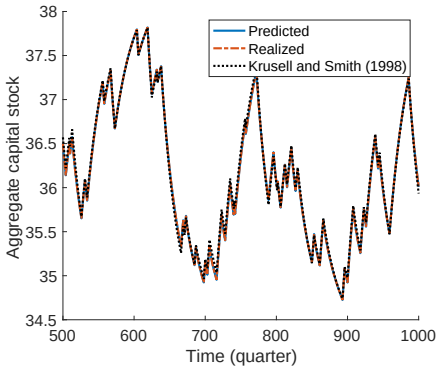

Notes: The figure plots the time series of the aggregate wealth (capital) K_t in the model of Krusell and Smith (1998). The line with a round tick mark is the predicted wealth time series (n^{th} guess) $\{K_t^{(n)}\}_{t=500}^{1000}$. The line with the square tick mark is the realized wealth time series $\{K_t^*\}_{t=500}^{1000}$. The dashed line is the predicted wealth time series implied by the law of motion in Krusell and Smith (1998).

this computational burden by using implied prices that converge to market clearing values in the limit of iterations.

To compare these approaches, I solve the Khan and Thomas (2008), using both the RTM and the Krusell and Smith (1997) algorithm its additional market-clearing loop. The substantial difference in computational efficiency complicates direct timing comparisons. Therefore, I instead evaluate both methods under identical dynamic consistency termination criteria. Figure C.3 plots the dynamics of price p_t (panel (a)) and aggregate capital stock K_t (panel (b)) computed from the RTM and Krusell and Smith (1997) algorithm. For the allocations computed from the RTM, both the predicted time series and the realized time series are plotted. As shown in the figure, all three lines display almost identical dynamics of the price and the aggregate allocations. The mean squared difference in the solutions between the RTM and Khan and Thomas (2008) is less than 10^{-5}.

In terms of the computational efficiency, the two methods display a substantial discrepancy. the RTM takes around 9 minutes to converge, while Krusell and Smith (1997) algorithm converge in around 5 to 6 hours on average in MATLAB.[15]

For both models of Krusell and Smith (1998) and Khan and Thomas (2008), I use the RTM using the sufficient statistic approach where the aggregate capital stock (the first moment) is used as the sufficient statistic. For this approach, it is necessary to check whether the firm's individual value (marginal value) function is strictly monotone in the aggregate capital stock. Figure C.4 and

[15]The convergence speed might change depending on the updating weight.

Figure C.3: Equilibrium allocation paths (Khan and Thomas, 2008)

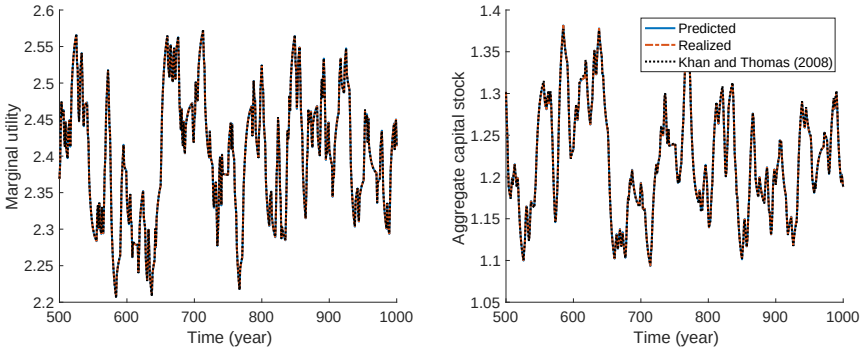

(a) Price p_t $(= 1/C_t)$ (b) Aggregate capital stocks K_t

Notes: The figure plots the time series of the price p_t the aggregate wealth (capital) K_t in the model of Khan and Thomas (2008). In both panels, the line with a round tick mark is the predicted time series (n^{th} guess) $\{p_t^{(n)}, K_t^{(n)}\}_{t=500}^{1000}$; the line with the square tick mark is the realized time series $\{p_t^*, K_t^*\}_{t=500}^{1000}$; the dashed line is the predicted time series implied by the law of motion.

C.5 show the strict monotonicity holds, which validates the aggregate capital stock's qualification for a sufficient statistic.

Figure C.4: Monotonicity of the marginal value functions in aggregate capital stock

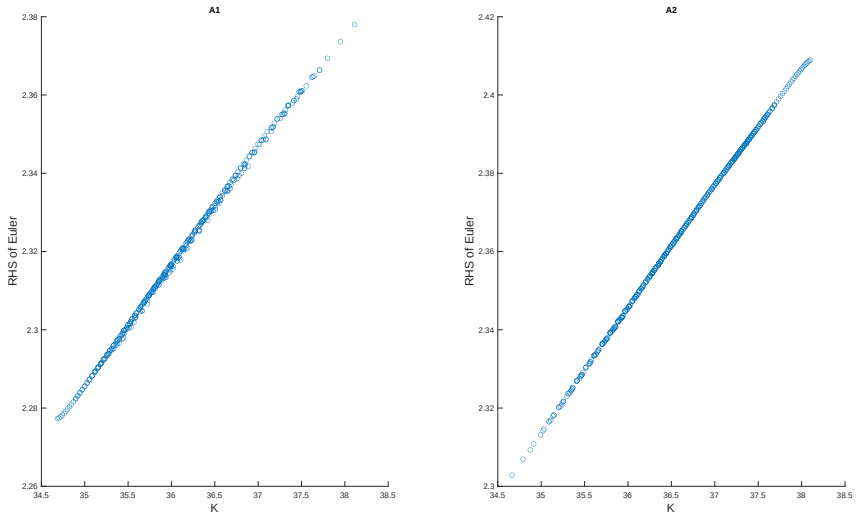

Figure C.4 plots the levels of the marginal benefit of the Euler equation in the vertical axis and the corresponding aggregate capital stock in the horizontal axis for an individual household with the median-level capital stock and the unemployed status (low idiosyncratic productivity) in the solution of Krusell and Smith (1998). Each panel is for different contemporaneous aggregate productivity levels. The monotonicity stays unaffected regardless of the choice of the individual

household.

Figure C.5: Monotonicity of the value functions in aggregate capital stock

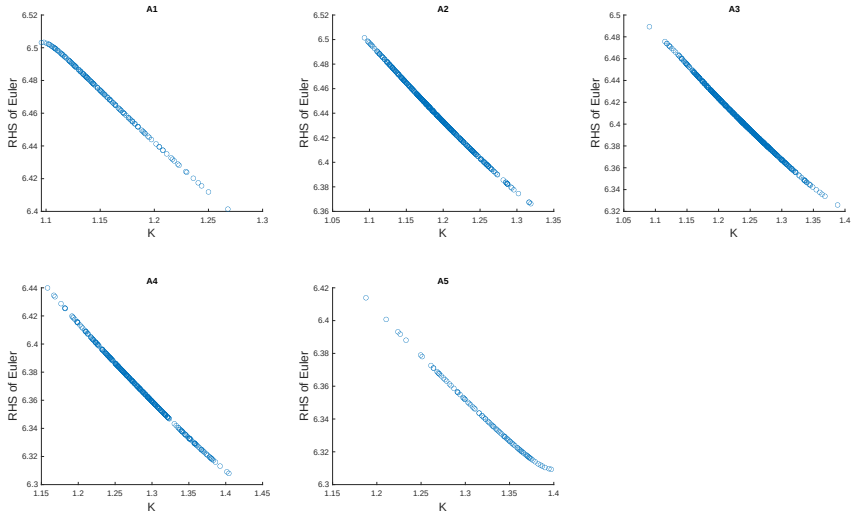

Figure C.5 plots the level of the value functions in the vertical axis and the the corresponding aggregate capital stock in the horizontal axis for an individual firm with the median-level capital stock and idiosyncratic productivity in the solution of Khan and Thomas (2008). Each panel is for the different contemporaneous aggregate productivity levels. The monotonicity stays unaffected regardless of the choice of the individual firm.

D Note on the leading applications

D.1 The leading application I: Krusell and Smith (1998) with endogenous labor supply, investment irreversibility, and fiscal spending shock

In the model, the market clearing is non-trivial as the wage determines individual labor supply, which needs to be aggregated instead of directly pinning down the aggregate labor supply.

$$\text{(Labor market)} \quad L(X) = \int zn(a, z; X) d\Phi \tag{7}$$

$$\text{(Capital market)} \quad K(X) = \int a d\Phi. \tag{8}$$

To illustrate this, I introduce an aggregate labor demand curve $\widetilde{L}$ and an individual labor supply curve $\widetilde{n}$, all of which include a price level $\widetilde{w}$ as an argument:

$$\begin{aligned} w(S) &= \arg_{\widetilde{w}} \left\{ \widetilde{L}(\widetilde{w}, X) - \int \widetilde{n}(a, z; \widetilde{w}, X) d\Phi = 0 \right\} \\ &= \arg_{\widetilde{w}} \left\{ \left(\frac{(1-\alpha)A}{\widetilde{w}} \right)^{\frac{1}{\alpha}} K - \int \left(\frac{z\widetilde{w}}{\eta c(a, z; \widetilde{w}, X)} \right)^{\chi} d\Phi = 0 \right\}. \end{aligned} \tag{9}$$

Line (9) follows from the first-order optimality conditions from the production sector (demand) and the household (supply). Given each wage level $\widetilde{w}$, the optimal consumption of the household needs to be specified, which requires an internal loop for clearing.[16] This fixed-point problem is computationally costly to solve. However, instead of the market clearing price, the repeated transition method uses the implied price w^*, as follows:

$$\begin{aligned} w^* &= \arg_{\widetilde{w}} \left\{ \widetilde{L}(\widetilde{w}, X) - \int \widetilde{n}(a, z; w^{(n)}, X) d\Phi = 0 \right\} \\ &= \arg_{\widetilde{w}} \left\{ \left(\frac{(1-\alpha)A}{\widetilde{w}} \right)^{\frac{1}{\alpha}} K - \int \left(\frac{zw^{(n)}}{\eta c(a, z; w^{(n)}, X)} \right)^{\chi} d\Phi = 0 \right\}. \end{aligned} \tag{10}$$

where $w^{(n)}$ is the guessed wage (predicted wage) in the n^{th} iteration. By bypassing the costly fixed-point problem, the method dramatically improves the speed of the computation.

From the first-order condition, the following inter-temporal optimality condition is obtained:

$$\frac{1}{c(a, z; X)} = \beta \mathbb{E}_{z,X} \left[\left(\frac{1}{c(a', z'; X')} \right) (1 + r(X')) - (1-\delta)\lambda(a', z'; X') \right] + \lambda(a, z; X) \tag{11}$$

where λ is the Lagrange multiplier of the irreversibility constraint. The left-hand side of the equation above is the marginal cost of saving in the unit of utility, and the right-hand side is the expected marginal value of saving. The marginal value includes contemporaneous gain out of relaxing today's constraint ($+\lambda(a, z; X)$) and the cost of tightening the future constraints ($-(1-\delta)\lambda(a', z'; X')$).

The expected marginal value requires the computation of state-contingent allocations (X' − *dependent*) of marginal utility $1/c$, capital rent r, and Lagrange multiplier λ.[17] In the computation of these terms, I employ the sufficient statistic approach described in Section 3, using aggregate capital stock $K(X)$ - the first moment of the individual wealth distribution - as the sufficient statistic.

[16] If a GHH utility is considered, this problem becomes trivial due to the missing wealth effect coming through the consumption in the denominator. However, the wealth effect is the key channel for the fiscal policy as will be demonstrated in the following section.

[17] The RTM computes the exact level of the Lagrange multiplier for the occasionally binding constraint at the individual level, which enables the accurate computation. The path of the lagrange multipliers is computed by the residuals using the Euler equation as in Rendahl (2014).

Figure D.6: Strict monotonicity of the marginal value in the aggregate capital stock

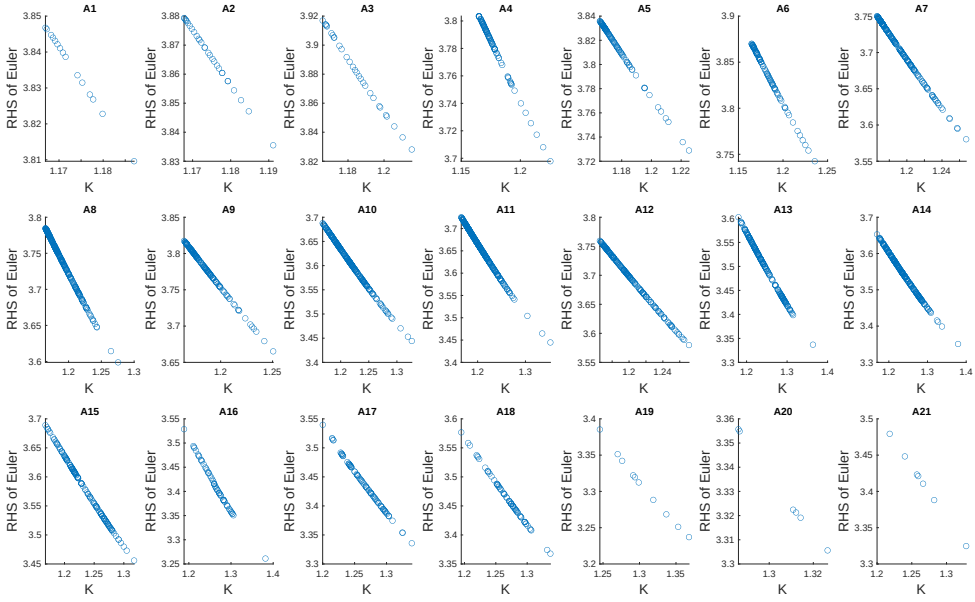

Notes: The figures are scatter plots of the marginal value functions in the vertical axis and the average capital as a sufficient statistic in the horizontal axis for different exogenous aggregate states (different panels) given the median level of individual wealth and productivity levels.

To validate this approach, I demonstrate that each individual's marginal value satisfies the strict monotonicity condition required by Proposition 1 across all aggregate exogenous state realizations. Figure D.6 provides graphical evidence, plotting marginal values against aggregate capital stock across different TFP and government demand levels $(A1, A2, A3, ..., A21)$ with individual states fixed at median levels of wealth and labor productivity. To systematically check the monotonicity, I compute the Spearman's coefficient between the sufficient statistic and the marginal value for each combination of individual states and exogenous aggregate states. The coefficient of unity implies the perfect monotonicity. In this analysis, the minimum coefficients among all combinations for both optimality conditions are distant from unity by 10^{-15}. The averages are not distinguishable from unity, and the standard deviations are around 10^{-16}. Thus, the monotonicity property holds robustly across the entire cross-section of the individual states.

For the computation, I use a 3,000-period simulation with independent aggregate TFP and government demand shocks. The TFP process is discretized using the Tauchen method with 7 grid points spanning three standard deviations, while the government demand shock uses 3 grid points covering one standard deviation. This yields 21 $(= 3 \times 7)$ total grid points for exogenous aggregate

state variations.

The irreversibility constraint parameter is from Guerrieri and Iacoviello (2015). The aggregate TFP process follows the same Markov chain as in Krusell and Smith (1998). The labor disutility parameter is calibrated to match the steady-state labor supply at 0.33. The parameter choices are based on annual frequency.

Table D.2: Parameters for the leading application I

Parameter	Description	Value
α	capital share	0.330
β	discount factor	0.960
δ	depreciation	0.100
ϕ	borrowing constraint parameter	0.975
η	Frisch elasticity	1.000
η	labor disutility	10.850
ρ	idiosyncratic productivity persistence	0.800
σ	idiosyncratic productivity volatility	0.014
$\overline{G}$	steady-state government demand	$0.200 * Y^{ss}$
ρ_A	aggregate TFP persistence	0.900
σ_A	aggregate TFP shock volatility	0.013
ρ_G	government demand persistence	0.800
σ_G	government demand shock volatility	$0.01 * Y^{ss}$

D.2 The leading application II: A heterogeneous-household RBC model of portfolio choice (Krusell and Smith, 1997) with endogenous labor supply

The model includes two inter-temporal assets, which necessarily leads to a highly complex endogenous aggregate state in equilibrium. Moreover, the model includes two occasionally binding constraints and the two non-trivial market clearing conditions for labor and bond market, which exponentially increases the computational burdens. Nevertheless, the RTM efficiently computes the global solution. I elaborate on the computational details in Appendix E.

The first-order conditions lead to two inter-temporal optimality conditions:

$$[\text{Risky asset}]: \quad \frac{1}{c(k,z;X)} = \beta \mathbb{E}_{z,X}\left[\left(\frac{1}{c(k',z';X')}\right)(1+r(X'))\right] + \lambda(k,z;X) \tag{12}$$

$$[\text{Safe asset}]: \quad \frac{1}{c(k,z;X)} = \beta \mathbb{E}_{z,X}\left[\left(\frac{1}{c(k',z';X')}\right)\right] + \psi(k,z;X) \tag{13}$$

where λ and ψ are Largrange multipliers for risky and safe assets' borrowing limit conditions,

respectively.

I take the sufficient statistic approach in Section 3, using the aggregate capital stock $K(X)$ - the first moment of the individual risky asset distribution - as the sufficient statistic. I validate this approach by checking the monotonicity condition of Proposition 1 for both of the inter-temporal optimality conditions (12) and (13), as reported in Figure D.7. Panel (a) and (b) are scatter plots of aggregate capital stock in the horizontal axis and the marginal values in the optimality condition in the vertical axis for different aggregate productivity realizations, given the median levels of individual wealth and labor productivity.[18] According to panel (a), the marginal value of the risky asset strictly monotonically decreases in aggregate capital K for each aggregate productivity, validating the sufficient statistic approach. Similarly, panel (b) reports the strict monotonicity for the safe asset. To systematically analyze the monotonicity, I compute the Spearman's coefficient between the sufficient statistic and the marginal value for each combination of individual states and exogenous aggregate states. From this analysis, I confirm that the minimum coefficients among all combinations for both optimality conditions are distant from unity by 10^{-5}. The averages are not distinguishable from unity, and the standard deviations are around 10^{-6}. Thus, the monotonicity property holds robustly across the entire cross-section of the individual states.

Figure D.7: Strict monotonicity of the marginal values in the aggregate capital stock

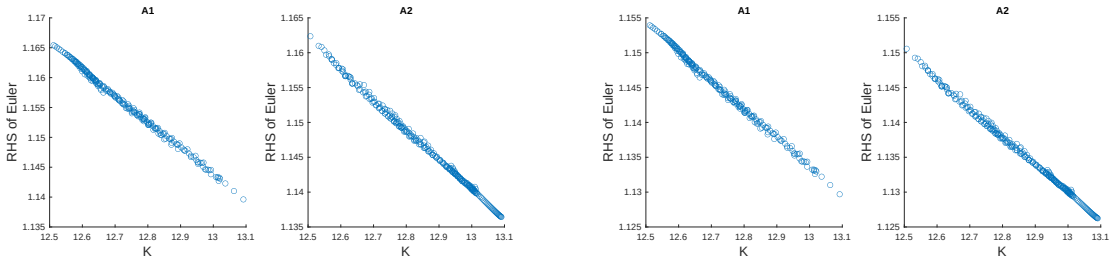

(a) Risky asset's inter-temporal optimality (b) Risk-free asset's inter-temporal optimality

Notes: The figures are scatter plots of the marginal value functions in the vertical axis and the average capital as a sufficient statistic in the horizontal axis for different exogenous aggregate states (different panels) given the median level of individual wealth and productivity levels. Panel (a) is for the marginal value of the risky asset, and panel (b) is for that of the risk-free asset.

The borrowing limit parameter and the aggregate TFP process are from Krusell and Smith (1997). The labor disutility parameter is calibrated to match the steady-state labor supply at 0.33. The parameter choices are based on quarterly frequency.

[18] As required by Proposition 1, the monotonicity needs to be checked for each individual state, which differs from the monotonicity along an individual's simulated state path.

Table D.3: Parameters for the leading application II

Parameter	Description	Value
α	capital share	0.360
β	discount factor	0.990
δ	depreciation	0.025
η	Frisch elasticity	1.000
η	labor disutility	8.000
ρ	idiosyncratic productivity persistence	0.900
σ	idiosyncratic productivity volatility	0.050
$\underline{b}$	borrowing limit for the risk-free asset	-2.400
$\overline{B}$	dummy bond term (only for computation)	20.000

E A heterogeneous-firm business cycle model with irreversible investment

In this section, I show that the repeated transition method is powerful in solving nonlinear DSGE models with heterogeneous agents. Specifically, I analyze a heterogeneous-firm real business cycle model where individual firms are subject to the occasionally binding capital irreversibility constraint.

The representative household maximizes the following lifetime utility in the recursive form:

$$\begin{aligned} V(a;X) = \max_{c,a',N} \; & log(c) - \eta N + \beta \mathbb{E} V(a';X') \\ \text{s.t.} \quad & c + \int M(X,X') a'(X') d\Gamma_{X'} = a + w(X)N \\ & X' = G_H(X) \end{aligned}$$

where c is consumption; a is the asset (equity) value before dividend payment; N is labor supply; M is the stochastic discount factor; w is wage; η is labor disutility parameter.[19] The aggregate state X is a bundle of the distribution of individual firms Φ and aggregate TFP A: $X = \{\Phi, A\}$. The representative agent rationally expects the law of motion G_H of the aggregate states. I use the apostrophe to indicate future allocations.

Heterogeneous firms solve the following maximization problem of the present value of the sum

[19] Following Khan and Thomas (2008), I assume the Frisch elasticity of the labor supply is infinity. However, the repeated transition method also applies to the case of the finite Frisch elasticity seamlessly. In the online appendix such examples are provided.

of the dividend stream in the recursive form:

$$\begin{aligned} J(k,z;X) = \max_{k'} \; & d + \mathbb{E}_{z,X} M(X,X') J(k',z';X') \\ \text{s.t. } & d = \pi(k,z;X) + (1-\delta)k - k' \\ & k' \geq \phi I_{ss} + (1-\delta)k \\ & \pi(k,z;X) = \max_{k,n} \; Ak^{\alpha} n^{\gamma} - w(X)n \\ & X' = G_F(X) \end{aligned}$$

where d is dividend; k is individual capital stock; z is the idiosyncratic productivity; n is the labor demand; π is a temporal profit; δ is the depreciation rate; I_{ss} is the steady-state aggregate investment level; ϕ is the irreversibility parameter. G_F is the law of motion of the aggregate state from a firm's perspective, which coincides with G_H under the rational expectation and satisfies the dynamic consistency in the recursive competitive equilibrium. The stochastic discount factor M is determined in the competitive market as follows:

$$M(X,X') = \beta \frac{c(X)}{c(X')}$$

The individual and aggregate log productivities follow AR(1) processes, which are discretized by the standard Tauchen method.

The recursive competitive equilibrium is defined based on the following market-clearing conditions:

$$\begin{aligned} \text{(Labor market)} \quad & N(X) = \int n(k,z;X) d\Phi \\ \text{(Equity market)} \quad & a(X) = \int J(k,z;X) d\Phi. \end{aligned}$$

In the market clearing condition, the supply of equity meets the demand in the form of household wealth.

For computation, I use the standard parameter levels in the literature, which are available in Appendix C. For easier computation, I normalize the firm's value function by contemporaneous consumption $c(S)$ following Khan and Thomas (2008). Then, I define a price $p(S) := 1/c(S)$ and the normalized value function $\tilde{J}(k,z;S) := p(S)J(k,z;S)$. From the intra-temporal and inter-temporal optimality conditions of households, $w(S) = \eta/p(S)$ and $M(S,S') = \beta p(S')/p(S)$. Thus, $p(S)$ is

the only price to characterize the equilibrium. Then, the equilibrium price $p(S)$ is determined from the following variant of the non-trivial market clearing condition:[20]

$$p = \arg_{\widetilde{p}} \left\{ 1/\widetilde{p} - \int \left[d(x; X, \widetilde{p}) + w(X, \widetilde{p}) n(x; X, \widetilde{p}) \right] d\Phi = 0 \right\}.$$

where the consumption is $c = 1/\widetilde{p}$. In the problem above, the individual dividend policy d, wage w, and labor demand n functions are augmented by an argument $\widetilde{p}$, indicating that these objects are calculated assuming the price is at the level of $\widetilde{p}$. This is a fixed-point problem and computationally costly to solve, as consumption $c = 1/\widetilde{p}$ affects the firms' inter-temporal decision, which in turn affects the dividend, consumption, and thus, $\widetilde{p}$. Instead of the market clearing price, the repeated transition method uses the implied price p^*, which is obtained as follows:

$$\begin{aligned} p^* &= \arg_{\widetilde{p}} \left\{ 1/\widetilde{p} - \int \left[d(x; X, p^{(n)}) + w(X, p^{(n)}) l(x; X, p^{(n)}) \right] d\Phi = 0 \right\} \\ &= 1/ \int \left[d(x; X, p^{(n)}) + w(X, p^{(n)}) l(x; X, p^{(n)}) \right] d\Phi, \end{aligned}$$

where $p^{(n)}$ is the guessed price in the n^{th} iteration. By bypassing the costly fixed-point problem, the method dramatically improves the speed of the computation.

The first-order condition of a firm's problem is as follows:[21]

$$1 = \mathbb{E}_{z,X} M(X, X') J_1(k', z'; X') + \lambda(k, z; X) \tag{14}$$

where λ is the Lagrange multiplier of the occasionally binding constraint. The envelope condition of a firm's problem is as follows:

$$\begin{aligned} J_1(k, z; X) &= \pi_1(k, z; X) + (1 - \delta) - \lambda(k, z; X)(1 - \delta) \\ &= \pi_1(k, z; X) + (1 - \delta)(1 - \lambda(k, z; X)) \end{aligned} \tag{15}$$

Combining equations (14) and (15), we have the following inter-temporal optimality condition:

$$1 - \lambda(k, z; X) = \underbrace{\mathbb{E}_{z,X} M(X, X') (\pi_1(k', z'; X') + (1 - \delta)(1 - \lambda(k', z'; X')))}_{\text{Expected marginal benefit}},$$

[20] This condition is derived from combining the household's budget constraint and the equity market clearing condition.

[21] The subscript denotes the partial derivative with respect to the argument in the corresponding argument order.

Figure E.8: Strict monotonicity of the marginal benefit in the aggregate capital stock

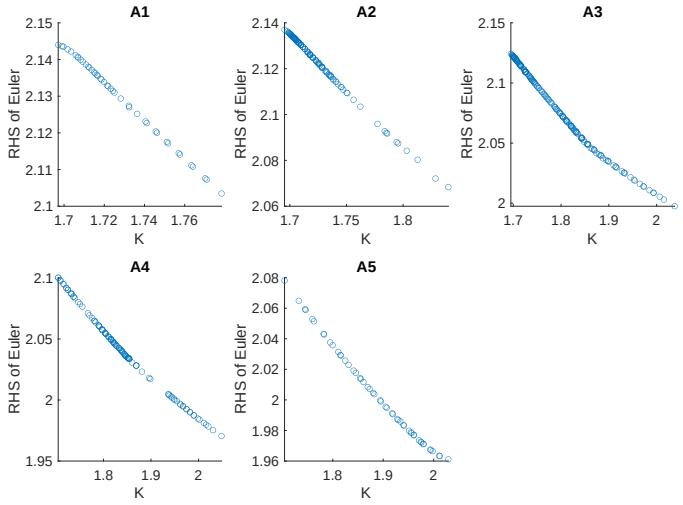

The expected marginal benefit requires the computation of state-contingent allocations (X' − *dependent*) of marginal profit π_1 and Lagrange multiplier λ. For this problem, I take the sufficient statistic approach, and the aggregate capital stock $K(S)$ (the first moment of the distribution of the firm-level capital stocks) is the sufficient statistic. I validate this approach by showing the monotonicity condition of Proposition 1 is satisfied. In particular, I show that each individual's marginal benefit $\pi_1 + (1-\delta)(1-\lambda)$ is strictly monotone in K for all aggregate exogenous state realization (TFP level). Figure E.8 plots the marginal benefit in the vertical axis and the corresponding aggregate equilibrium capital stock in the horizontal axis for different TFP levels ($A1$, $A2$, $A3$, ..., $A7$) given the individual state fixed at the median levels of capital stock and the firm-level productivity. In the unreported tests, which are available in the sample code, I confirm that monotonicity holds regardless of the choice of an individual firm.

For the computation, I run a simulation of 1,000 periods of aggregate TFP shock, where the TFP is discretized by the Tauchen method, covering the two standard deviation ranges. The computed aggregate capital path is highly nonlinear due to the occasionally binding constraint. Figure E.9 plots a part of the predicted path $\{K_t^{(n)}\}_{t=0}^T$ and the realized (implied) path $\{K_t^*\}_{t=0}^T$ of aggregate capital K_t obtained from the repeated transition method and the simulated path from the fitted log-linear law of motion. While the predicted path and the realized path coincide at the equilibrium path, the log-linear prediction significantly deviates from the others.

Figure E.9: The equilibrium path of aggregate capital stock

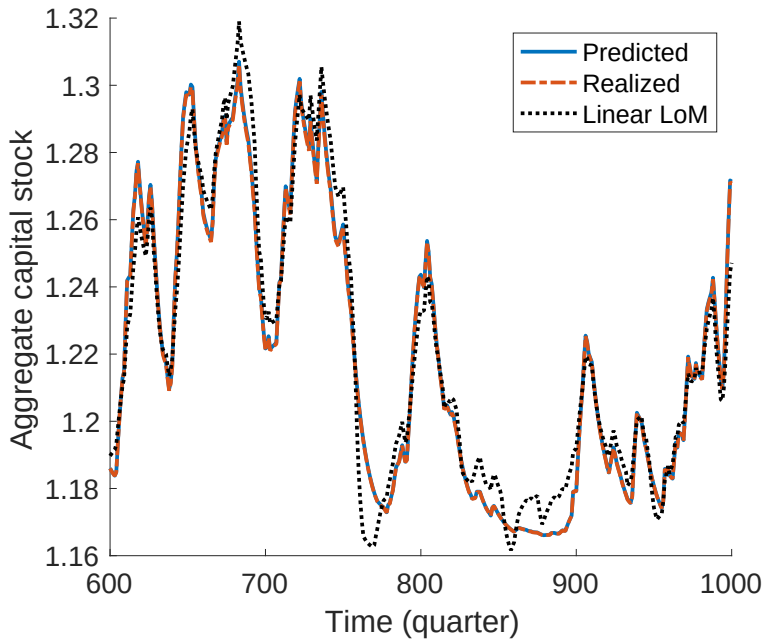

E.1 Nonlinearity and aggregation

In this section, I compare the nonlinearity implied in the heterogeneous firm model with the one in the representative firm model, which is obtained by simply muting the heterogeneous firm-level productivity.[22] For a valid comparison, I feed the same exogenous aggregate TFP path for both models and compute the equilibrium using the repeated transition method. Figure E.10 plots a part of the equilibrium capital path of the heterogeneous firm model (solid line) and the representative firm model (dash-dotted line) in log deviation from each model's steady state.

The volatility of the aggregate capital stock is significantly greater in the heterogeneous firm model, which is the by-product of the greater volatility in the aggregate investment. Table E.4 reports the business cycle statistics of the two models. The output and investment are around 10 percent more volatile in the heterogeneous firm model than the other, while consumption volatilities are at a similar level. The skewness of output is greater, and the skewness of consumption and investment is lower in the heterogeneous firm model.

The representative firm model fails to represent the heterogeneous-firm model over the business cycle. The reason is the nonlinearity at the firm-level capital dynamics.[23] To see this, I compute

[22] All the parameters are assumed at the same level except for the firm-level productivity.

[23] This result is specific to this model. For example, Khan and Thomas (2008) shows that the general equilibrium effect washes out the firm-level nonlinearity in their model.

Figure E.10: Equilibrium dynamics comparison: Heterogeneous vs. representative

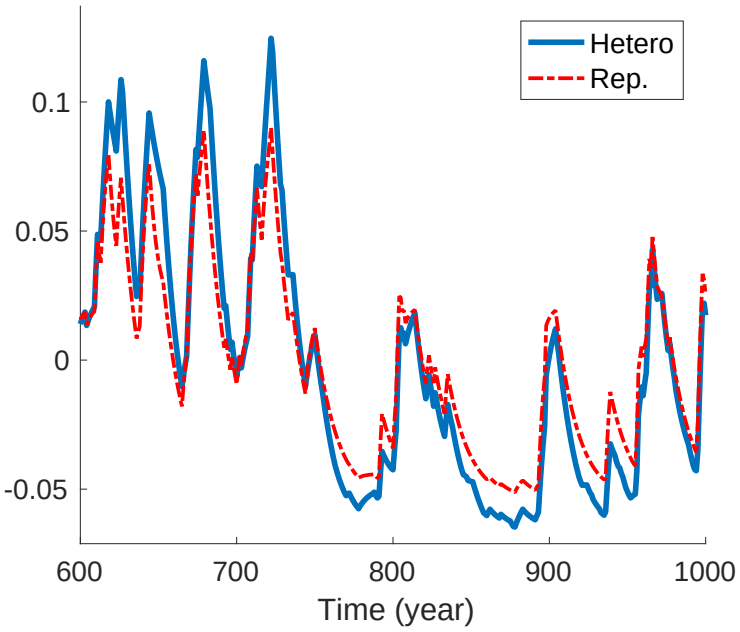

Table E.4: Business cycle statistics: Heterogeneous vs. representative

	Heterogeneous	Representative
Volatility		
$log(Output)$	0.042	0.039
$log(Consumption)$	0.034	0.034
$log(Investment)$	0.083	0.077
Skewness		
$log(Output)$	0.672	0.638
$log(Consumption)$	-0.049	-0.02
$log(Investment)$	1.757	1.926

the same heterogeneous and representative firm models without the occasionally binding constraint (fully reversible investment), which is the source of the nonlinearity. I refer to this version as the frictionless benchmark. Figure E.11 plots the aggregate capital dynamics of the frictionless benchmark of both models in log deviation from the steady state and the predicted path by the log-linear law of motion. These three lines perfectly coincide indicating that firm-level linearity

Figure E.11: Equilibrium dynamics comparison - frictionless: Heterogeneous vs. representative

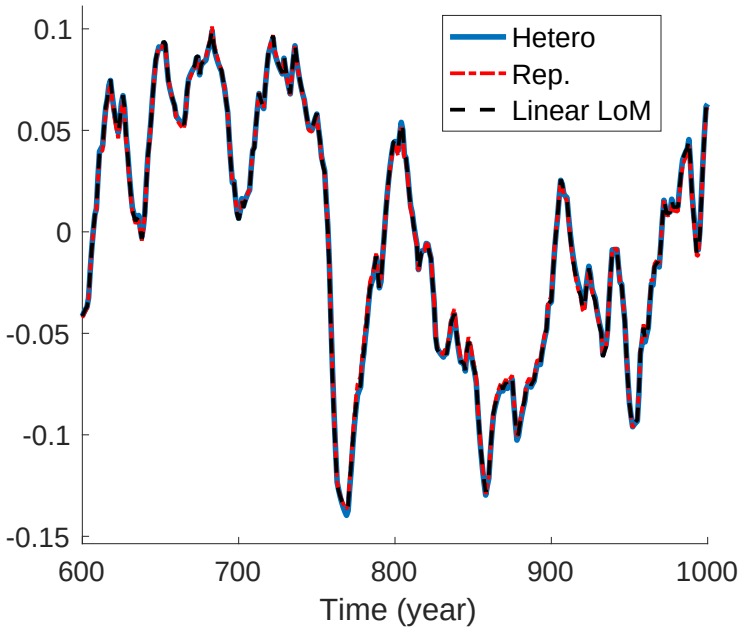

makes the perfect representation that is also linear.[24]

[24]The relevance of the firm-level nonlinearity in this model is contrasted with the neutrality result of Veracierto (2002). However, the two results are based on different firm-level setups, so the direct comparison is limited: the leading application is based on the occasionally-binding irreversibility constraint, while Veracierto (2002) features an (S, s) cycle in the firm-level capital stock.

E.2 Parameters used for the heterogeneous-firm business cycle model with irreversible investment

Table E.5: Parameters for the heterogeneous-firm business cycle model with irreversible investment

Parameter	Description	Value
α	capital share	0.256
γ	labor share	0.640
δ	depreciation	0.069
ϕ	borrowing constraint parameter	0.975
β	discount factor	0.977
η	labor disutility	2.400
ρ	idiosyncratic productivity persistence	0.859
σ	idiosyncratic productivity volatility	0.022
ρ_A	aggregate TFP persistence	0.859
σ_A	aggregate TFP volatility	0.014

All the parameters are from Khan and Thomas (2008) except for the irreversibility constraint parameter, which I used the level of Guerrieri and Iacoviello (2015).

F A note on the bond market clearing condition in the extended model of Krusell and Smith (1997)

The net zero bond supply condition in the leading application II Krusell and Smith (1997) leads to non-invertible identity:

$$q^b(X)B' = B \iff q^b(X) \times 0 = 0. \tag{16}$$

Therefore, it is demanding to specify the implied price q_t^{b*} in the bond market. To overcome this issue, I introduce a dummy bond $\overline{B} > 0$ such that

$$q_t^{b*}\overline{B} := Y_t^{(n)} - C_t^* - I_t^* - B_t^* + q_t^{b(n)}\overline{B} \implies q_t^{b*} = \frac{Y_t^{(n)} - C_t^* - I_t^* - B_t^* + q_t^{b(n)}\overline{B}}{\overline{B}}. \tag{17}$$

n equilibrium, the national accounting identity must hold. During the iterative solution process, any discrepancy between the implied output Y_t^* and the n^{th}-guess $Y_t^{(n)}$ provides valuable information for updating the bond price $q_t^{b(n)}$ to satisfy this identity given the n^{th}-guess $q_t^{b(n)}$. [25] This price adjustment mechanism requires a dummy bond as an anchor point for relative price updates. Without this reference asset (i.e., if the dummy bond value were zero), there would be no basis for calibrating the bond price adjustments needed to satisfy market clearing conditions.

This approach can be generally used to pin down the implied price level required for non-trivial market clearing conditions under net zero supply. By contrast, state-space-based approaches directly solve for the market clearing price (q_t^b) at the exact point where supply and demand curves intersect at zero, eliminating the need for this dummy bond.

[25] The information gain does not necessarily have to come from the output. In an unreported result, I found the difference in consumption also provides identifying variation for the implied bond price.

G Heterogeneous portfolio adjustment over the business cycle for different labor income groups

The global nonlinear solution of the model reveals a novel prediction about heterogeneous portfolio adjustment across households. Figure G.12 illustrates this heterogeneity by tracking the household-level average of the risky asset weight in the portfolio for two groups: high-productivity households (defined as those in the top tercile of the productivity distribution) and low-productivity households (those in the bottom tercile), plotted against output deviations from steady state.

Both groups' households display counter-cyclical portfolio adjustments, increasing their risky asset allocations with a one-period lag relative to output fluctuations. However, the magnitude of these adjustments differs markedly across productivity levels: low-productivity households exhibit substantially more aggressive rebalancing behavior, with portfolio volatility more than 4 times greater than that of high-productivity households.

Figure G.12: The equilibrium paths of risky asset portion: high vs. low productivity households

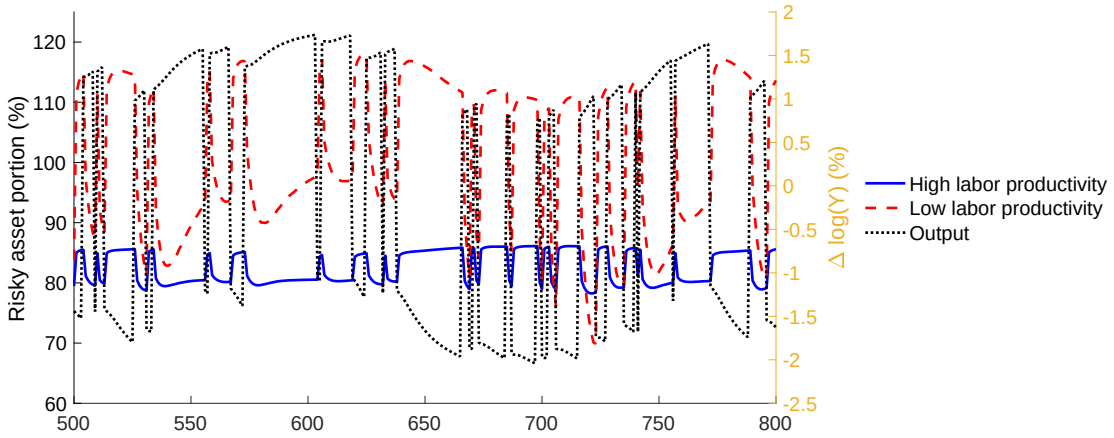

Notes: The figure plots the time series of the risky asset portion (%) in the wealth portfolio for different households in the extended model of Krusell and Smith (1997). The solid line represents households in the top productivity tercile, while the dashed line shows households in the bottom productivity tercile. The dotted line depicts output (measured as percentage deviation from steady state), with values shown on the secondary vertical axis at the right side of the figure.

The group-level total asset composition dynamics are also starkly different. Figure G.13 contrasts the asset holdings of high and low productivity groups against output deviations from steady state, with panel (a) showing risky asset holdings and panel (b) displaying risk-free asset positions. Panel (a) demonstrates that low productivity households maintain larger risky asset positions than their high productivity counterparts, with more pronounced pro-cyclical variation. Panel (b) re-

veals the financing strategy behind these positions: low productivity households achieve their large risky asset holdings through aggressive leverage, maintaining risk-free borrowing positions consistently near the constraint ($\underline{b} = -2.4$). In contrast, high productivity households hold large and stable risk-free asset positions throughout the business cycle.

These patterns offer important insights for both inequality dynamics and asset pricing theory. The RTM solution reveals how the bond market mediates heterogeneous hedging motives across household types, generating highly nonlinear and volatile bond prices. This interaction between household heterogeneity and financial markets provides new perspectives on both inequality transmission and asset pricing mechanisms.

Figure G.13: Risky and risk-free asset dynamics: high and low productivity

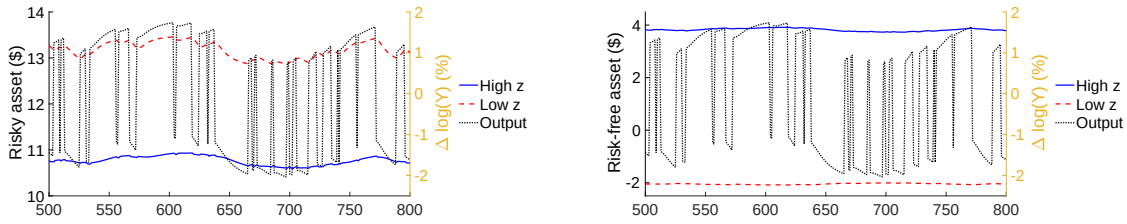

(a) Risky asset dynamics

(b) Risk-free asset dynamics

Notes: The figure plots the time series of the different asset holdings ($) by household types in the extended model of Krusell and Smith (1997). Panel (a) is for the risky asset, and panel (b) is for the risk-free asset. The solid line represents households in the top productivity tercile, while the dashed line shows households in the bottom productivity tercile. The dotted line depicts output (measured as percentage deviation from steady state), with values shown on the secondary vertical axis at the right side of the figure.

References

Azinovic, M., L. Gaegauf, and S. Scheidegger (2022). Deep equilibrium nets. *International Economic Review 63*(4), 1471–1525.

Cao, D., W. Luo, and G. Nie (2023, January). Global DSGE Models. *Review of Economic Dynamics*, S1094202523000017.

Christiano, L. J. and J. D. Fisher (2000). Algorithms for solving dynamic models with occasionally binding constraints. *Journal of Economic Dynamics and Control 24*(8), 1179–1232.

Den Haan, W. J. (2010, January). Assessing the accuracy of the aggregate law of motion in models with heterogeneous agents. *Journal of Economic Dynamics and Control 34*(1), 79–99.

Fernández-Villaverde, J., S. Hurtado, and G. Nuño (2023). Financial frictions and the wealth distribution. *Econometrica 91*(3), 869–901.

Guerrieri, L. and M. Iacoviello (2015, March). OccBin: A toolkit for solving dynamic models with occasionally binding constraints easily. *Journal of Monetary Economics 70*, 22–38.

Han, J., Y. Yang, and W. E (2025). DeepHAM: A Global Solution Method for Heterogeneous Agent Models with Aggregate Shocks. *Working Paper*, 38.

Judd, K. L. (1992, December). Projection methods for solving aggregate growth models. *Journal of Economic Theory 58*(2), 410–452.

Khan, A. and J. K. Thomas (2008, March). Idiosyncratic Shocks and the Role of Nonconvexities in Plant and Aggregate Investment Dynamics. *Econometrica 76*(2), 395–436.

Krusell, P. and A. A. Smith, Jr. (1997, June). Income and Wealth Heterogeneity, Portfolio Choice, and Equilibrium Asset Returns. *Macroeconomic Dynamics 1*(02).

Krusell, P. and A. A. Smith, Jr. (1998, October). Income and Wealth Heterogeneity in the Macroeconomy. *Journal of Political Economy 106*(5), 867–896.

Maliar, L., S. Maliar, and F. Valli (2010, January). Solving the incomplete markets model with aggregate uncertainty using the Krusell–Smith algorithm. *Journal of Economic Dynamics and Control 34*(1), 42–49.

McGrattan, E. R. (1996). Solving the stochastic growth model with a finite element method. *Journal of Economic Dynamics and Control 20*(1), 19–42.

Rendahl, P. (2014, 06). Inequality Constraints and Euler Equation-Based Solution Methods. *The Economic Journal 125*(585), 1110–1135.

Veracierto, M. L. (2002, March). Plant-level irreversible investment and equilibrium business cycles. *American Economic Review 92*(1), 181–197.

Young, E. R. (2010, January). Solving the incomplete markets model with aggregate uncertainty using the Krusell-Smith algorithm and non-stochastic simulations. *Journal of Economic Dynamics and Control 34*(1), 36–41.